

## *Electronic Supporting Information*

# **Syntheses and structures of a new 2D layered borate and a novel 3D porous-layered alunminoborate**

Chong-An Chen,<sup>a</sup> Rui Pan<sup>a</sup> and Guo-Yu Yang<sup>\*a,b</sup>

<sup>a</sup>MOE Key Laboratory of Cluster Science, School of Chemistry and Chemical Engineering, Beijing Institute of Technology, Beijing 100081, China. <sup>b</sup>College of Chemistry, Fuzhou University, Fuzhou, Fujian 350108, China. E-mail: [ygy@bit.edu.cn](mailto:ygy@bit.edu.cn), [ygy@fjirsm.ac.cn](mailto:ygy@fjirsm.ac.cn). Fax: (+86) 10-6891-8572

**Table S1.** Hydrogen bond distances (Å) and angles (°) for the compound **1**.

**Table S2.** Hydrogen bond distances (Å) and angles (°) for the compound **2**.

**Figure S1.** The PXRD patterns of **1** and **2**, respectively.

**Figure S2.** Hydrogen bonds between 1,2-dap molecule and inorganic framework in **1**.

**Figure S3.** View of different B<sub>7</sub> FBBs: a) [B<sub>7</sub>O<sub>9</sub>(OH)<sub>5</sub>]<sup>2-</sup>; b) [B<sub>7</sub>O<sub>9</sub>(OH)<sub>6</sub>]<sup>3-</sup>; c) [B<sub>7</sub>O<sub>10</sub>(OH)<sub>3</sub>]<sup>2-</sup>; d, e) [B<sub>7</sub>O<sub>12</sub>(OH)<sub>3</sub>]<sup>2-</sup>; f) [B<sub>7</sub>O<sub>12</sub>(OH)<sub>4</sub>]<sup>7-</sup>; g) [B<sub>7</sub>O<sub>14</sub>]<sup>7-</sup>; h) [B<sub>7</sub>O<sub>14</sub>(OH)<sub>2</sub>]<sup>9-</sup>; i) [B<sub>7</sub>O<sub>15</sub>]<sup>9-</sup>; j) [B<sub>7</sub>O<sub>15</sub>(OH)<sub>2</sub>]<sup>11-</sup>; k) [B<sub>7</sub>O<sub>16</sub>]<sup>11-</sup>; l) [B<sub>7</sub>O<sub>17</sub>]<sup>13-</sup>; m) [B<sub>7</sub>O<sub>13</sub>(OH)]<sup>6-</sup> (This work).

**Figure S4.** View of compositions of channel E (a), F (b) and G (c).

**Figure S5.** The metal ions positions in the inorganic framework in **2**.

**Figure S6.** View of FBB (a), 2D monolayer (b), porous layer (c), channel system (d) three types of 14-MR channels (e, f and g) in **3**.

**Figure S7.** a) The [Al<sub>2</sub>B<sub>8</sub>O<sub>20</sub>(OH)<sub>2</sub>]<sup>12-</sup> dimeric cluster in **4**; b) View of 3D porous layer of **4**; (c) The three types of 14-MR channels (A, B and C); d) The intercommunicated channel system in **4**.

**Figure S8.** The TG curves of **1** and **2**, respectively.

**Figure S9.** IR spectra of **1** and **2**, respectively.

**Table S1.** Hydrogen bond distances (Å) and angles (°) for the compound **1**.

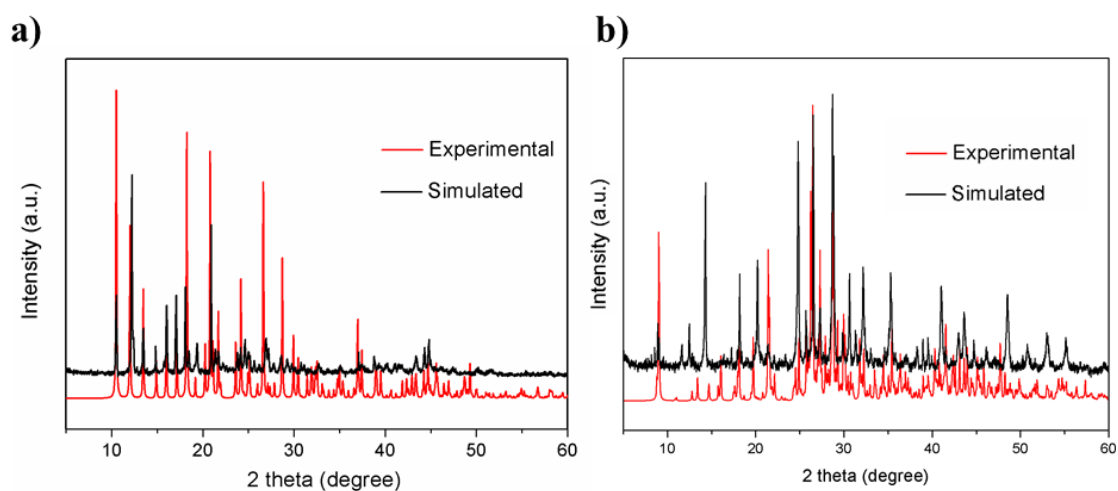
D–H···A	d(D–H)	d(H···A)	d(D···A)	∠(DHA) (°)
N(1)–H(1A)···O(8)#1	0.89	1.96	2.827(3)	163.0
N(1)–H(1B)···O(1)#1	0.89	2.45	3.170(3)	138.0
N(1)–H(1B)···O(2)#1	0.89	2.27	3.107(3)	157.5
N(1)–H(1C)···O(7)#2	0.89	2.17	2.958(3)	147.0
N(1)–H(1C)···O(10)#2	0.89	2.48	3.151(3)	132.6
N(2)–H(2B)···O(7)#4	0.89	1.94	2.811(4)	160.0
N(2)–H(2C)···O(8)#5	0.89	2.22	2.990(3)	145.0
N(2)–H(2C)···O(9)#5	0.89	2.41	3.165(3)	143.6
N(2)–H(2A)···O(11)#3	0.89	2.37	3.222(3)	160.0
O(6)–H(6A)···O(5)#4	0.82	1.95	2.766(3)	177.0
C(1)–H(1E)···O(3)#2	0.97	2.42	3.325(3)	155.0
C(2)–H(4)···O(9) #5	0.96	2.47	3.296(5)	143.0

**Symmetric codes:** #1: 1-x,1-y,2-z; #2: 1/2-x,1/2+y,3/2-z; #3: x,1+y,z; #4: 1-x,1-y,1-z; #5: 3/2-x,1/2+y,3/2-z.

**Table S2.** Hydrogen bond distances (Å) and angles (°) for the compound **2**.

D–H···A	d(D–H)	d(H···A)	d(D···A)	∠(DHA) (°)
O(1)–H(1)···O(24)#1	0.77	2.08	2.845(6)	177.0

**Symmetric codes:** #1: 1+x,y,z

**Figure S1.** The PXRD patterns of **1** and **2**, respectively.

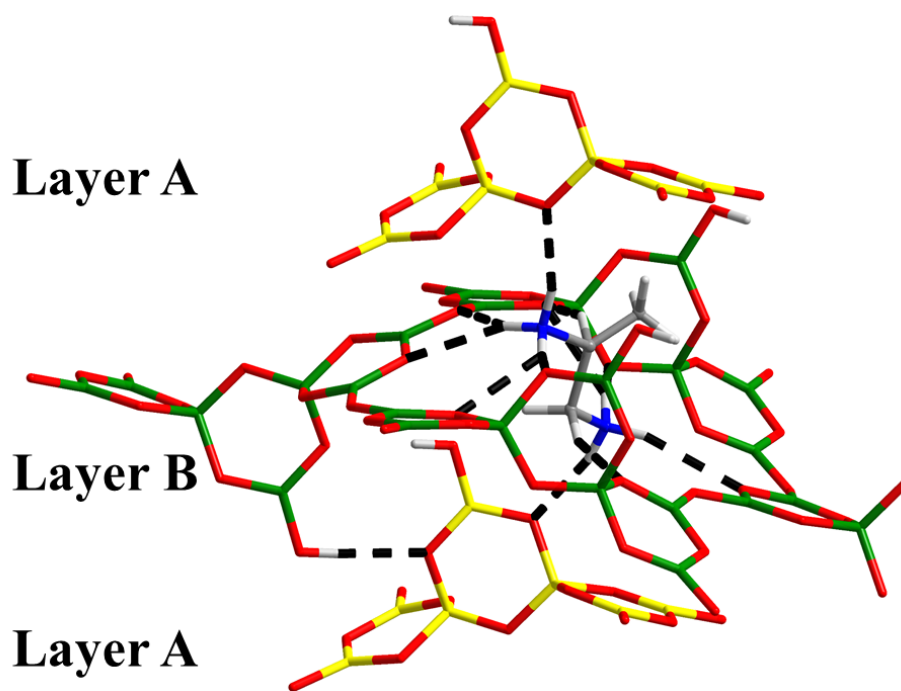


**Figure S2.** Hydrogen bonds between 1,2-dap molecule and inorganic framework in **1**.

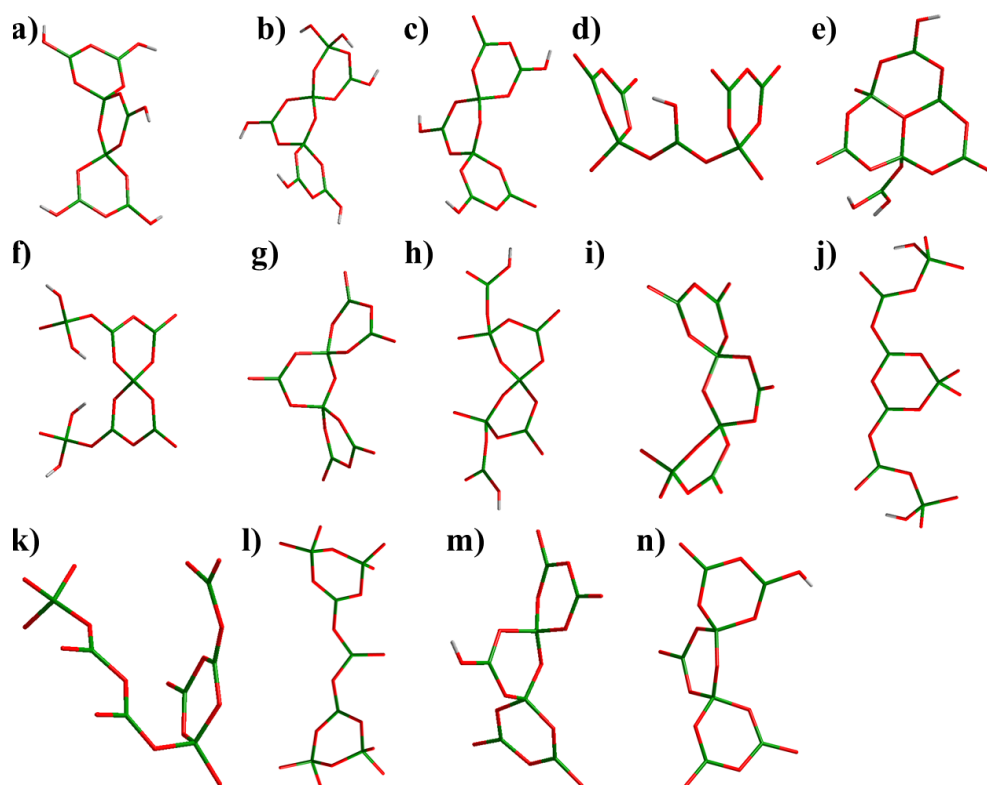


**Figure S3.** View of different B<sub>7</sub> FBBs: a) [B<sub>7</sub>O<sub>9</sub>(OH)<sub>5</sub>]<sup>2-</sup> ([7:(5Δ+2T)]); b) [B<sub>7</sub>O<sub>9</sub>(OH)<sub>6</sub>]<sup>3-</sup> ([7:(4Δ+3T)]); c) [B<sub>7</sub>O<sub>10</sub>(OH)<sub>3</sub>]<sup>2-</sup> ([7:(5Δ+2T)]); d,e) [B<sub>7</sub>O<sub>12</sub>(OH)<sub>3</sub>]<sup>2-</sup> ([7:(3:2Δ+1T) + (1:Δ) + (3:2Δ+1T)]) and [7:(6:3Δ+3T) + (1:Δ)]; f) [B<sub>7</sub>O<sub>12</sub>(OH)<sub>4</sub>]<sup>7-</sup> ([7:(1:T) + (5:4Δ+1T) + (1:T)]); g) [B<sub>7</sub>O<sub>14</sub>]<sup>7-</sup> ([7:(1:T) + (5:4Δ+1T) + (1:T)]); h) [B<sub>7</sub>O<sub>14</sub>(OH)<sub>2</sub>]<sup>9-</sup> ([7:(1:Δ) + (5:2Δ+3T) + (1:Δ)]); i) [B<sub>7</sub>O<sub>15</sub>]<sup>9-</sup> ([7:(4Δ+3T)]); j) [B<sub>7</sub>O<sub>15</sub>(OH)<sub>2</sub>]<sup>11-</sup> ([7:(2:Δ+T) + (3:2Δ+T) + (2:Δ+T)]); k) [B<sub>7</sub>O<sub>16</sub>]<sup>11-</sup> ([7:(3:2Δ+T) + (3:2Δ+T) + (1:Δ)]); l) [B<sub>7</sub>O<sub>17</sub>]<sup>13-</sup> ([7:(3:Δ+2T) + (1:Δ) + (3:Δ+2T)]); m) [B<sub>7</sub>O<sub>13</sub>(OH)]<sup>6-</sup> ([7:(5Δ+2T)]) in **1** (This work). n) [B<sub>7</sub>O<sub>13</sub>(OH)]<sup>6-</sup> ([7:(5Δ+2T)]) in **2** (This work).

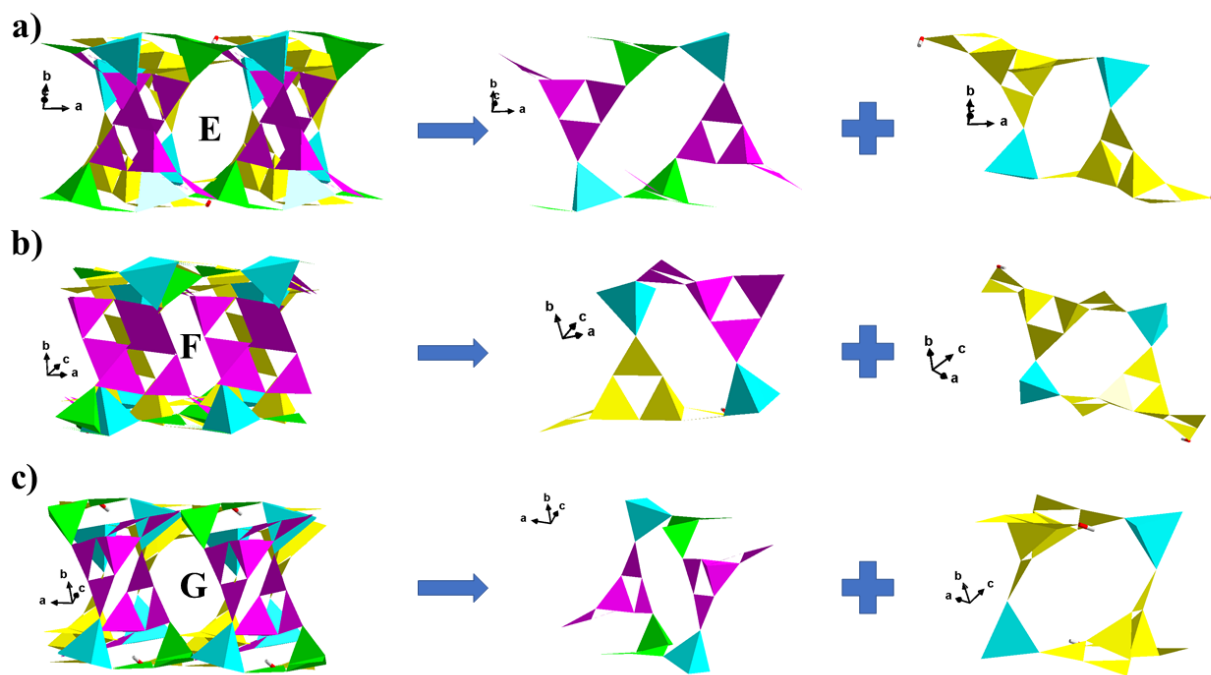


Figure S4. View of compositions of channel E (a), F (b) and G (c).

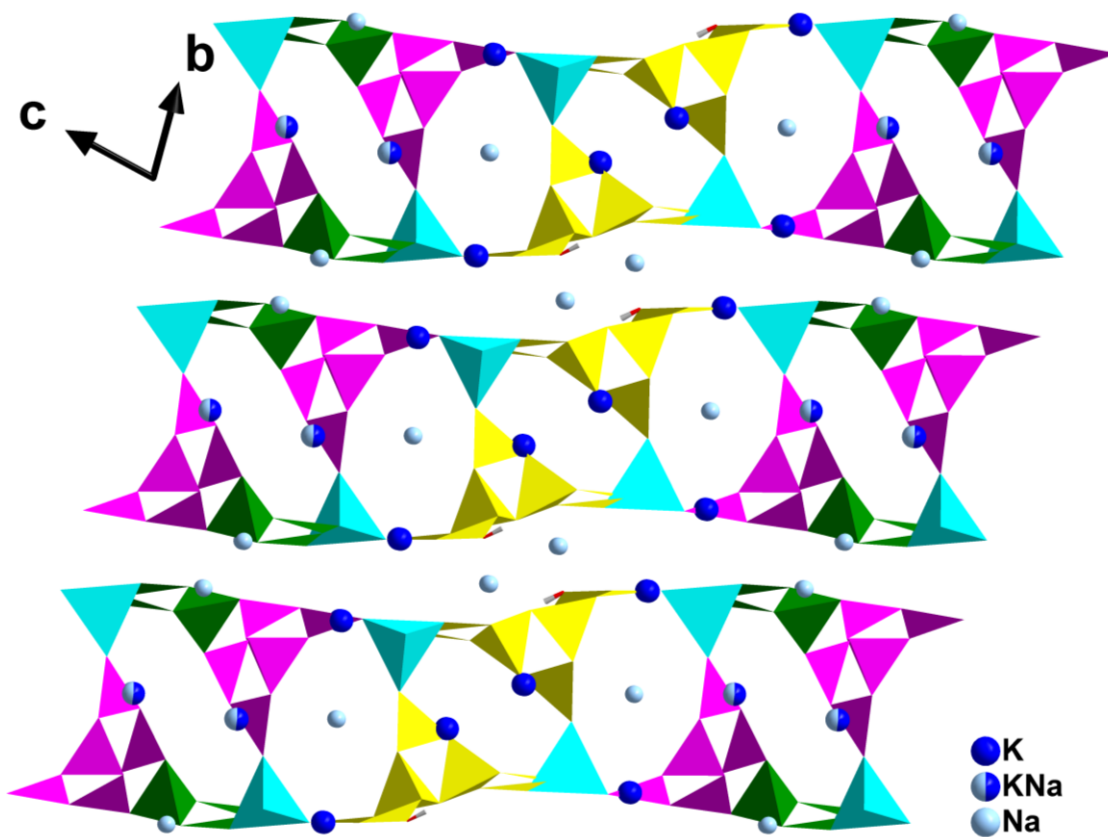
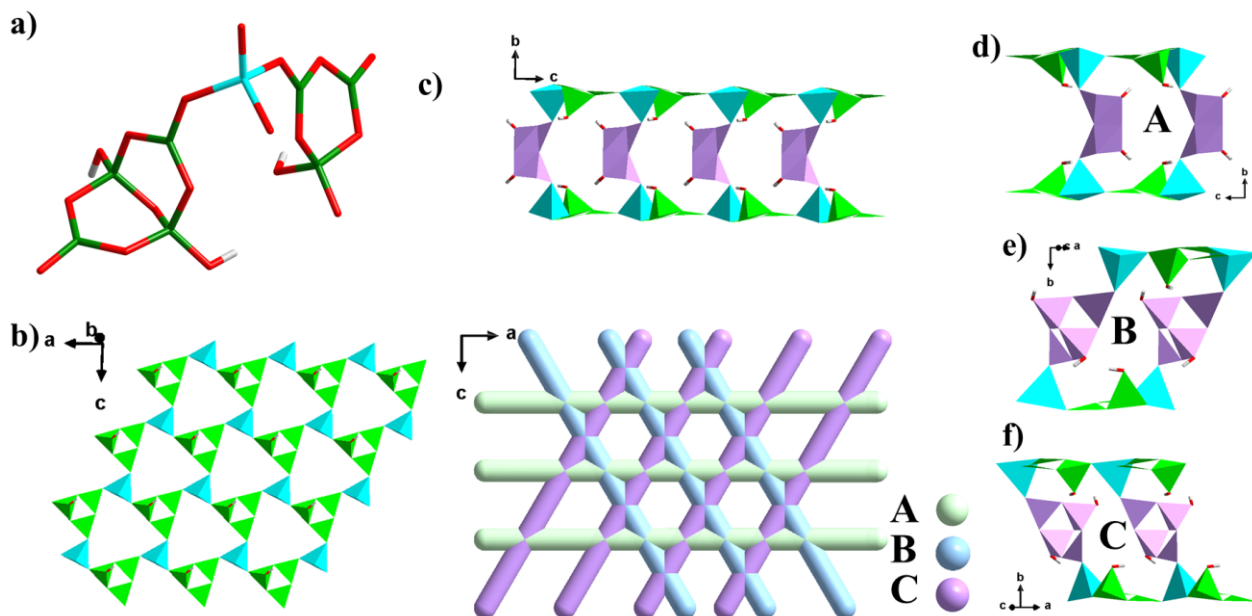
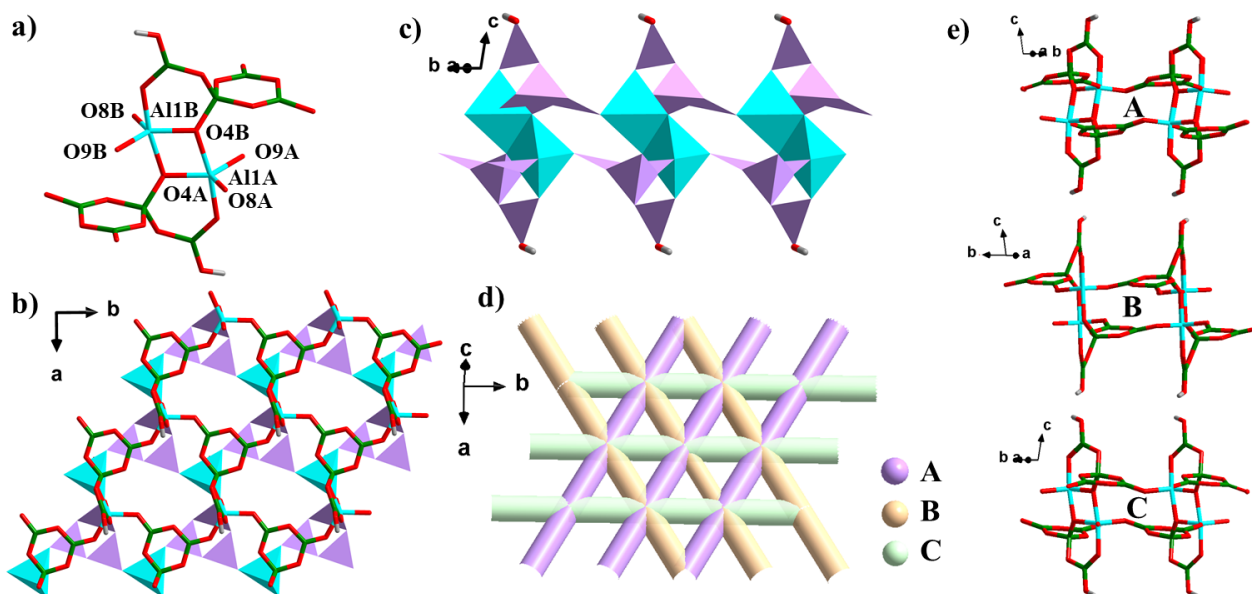


Figure S5. The metal ions positions in the inorganic framework in 2.



**Figure S6.** View of a) *FBB*; b) 2D ABO monolayer; c) 3D ABO porous layer; d) The intercommunicated channel system; e, f, g) Three types of 14-MR channels in **3**.



**Figure S7.** a) The  $[Al_2B_8O_{20}(OH)_2]^{12-}$  dimeric clusters in **4**; b) Top view of 3D porous layer showing interlaced 9-MR windows in **4**; (c) Side view of 3D porous layer; d) The intercommunicated channel system of **4** (A, B and C); e) The three types of 6-MR windows along the  $[010]$ ,  $[110]$  and  $[1-10]$  directions, respectively.

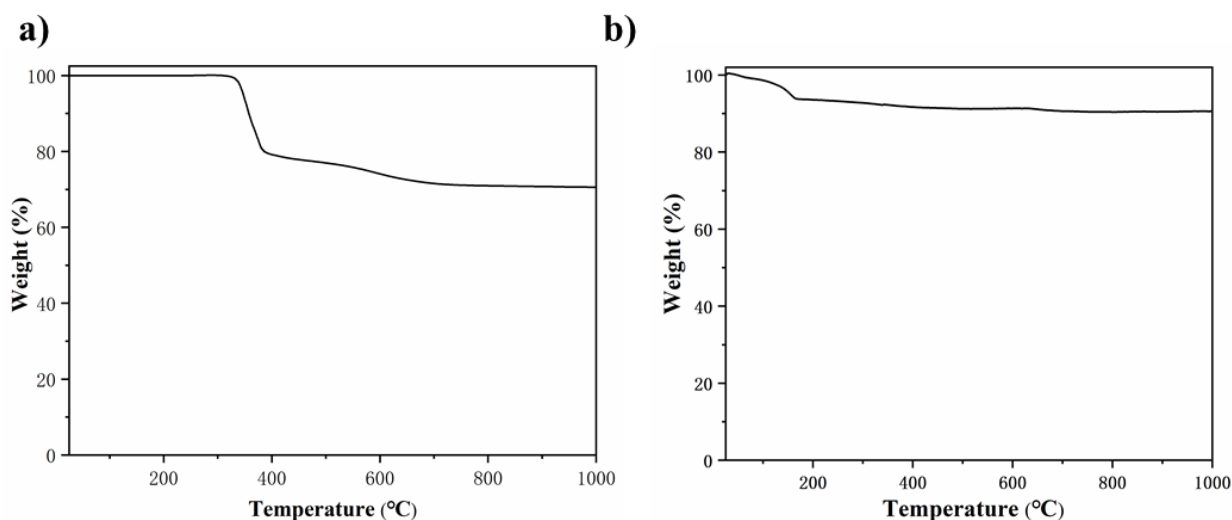


**Figure S8.** The TG curves of **1** and **2**, respectively.

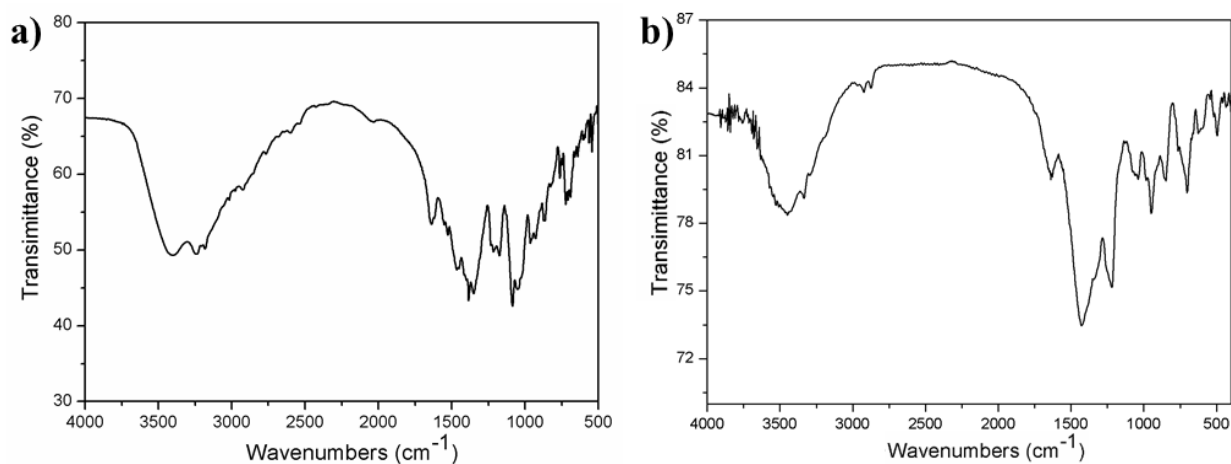


**Figure S9.** IR spectra of **1** and **2**, respectively.

As shown in Fig. S9, for **1**, the bands around  $3400\text{ cm}^{-1}$  are the characteristic peaks of the asymmetric stretching vibrations of O-H, N-H and C-H bonds. The bands appear at  $1662\text{-}1607\text{ cm}^{-1}$  belong to the bending vibrations of O-H, N-H and C-H bonds. The absorption peaks from  $1483\text{-}1336\text{ cm}^{-1}$  are attributed to the asymmetrical stretching vibrations of  $\text{BO}_3$  triangles, while the peaks ranging from  $1148\text{-}985\text{ cm}^{-1}$  are the asymmetrical stretching peaks of  $\text{BO}_4$  tetrahedrons. For **2**, the absorption peaks occurring from  $3452\text{-}3172\text{ cm}^{-1}$  are the asymmetric stretching vibrations of O-H bonds. The peak at  $1637\text{ cm}^{-1}$  and  $1465$  are the characteristic peaks of C-O bonds, which confirm the existence of  $\text{CO}_3^{2-}$ .<sup>[1-2]</sup> The peaks appear in the range of  $1465\text{-}1210\text{ cm}^{-1}$  and  $1058\text{-}942\text{ cm}^{-1}$  are the asymmetric stretching vibrations of  $\text{BO}_3$  and  $\text{BO}_4$ , respectively. The bands in the region of  $740\text{-}900\text{ cm}^{-1}$  are the Al-O stretching vibrations of tetrahedral  $\text{AlO}_4$  groups.

[1] Z. H. Cheng, A. Yasukawa, K. Kandori and T. Ishikawa. *Langmuir*, 1998, **14**, 6681-6686.

[2] J. A. Toledo-Antonio, S. Capula, M. Antonia Corte's-Ja'come, C. Angeles-Cha'vez, E. Lo'pez-Salinas, G. Ferrat, J. Navarrete and J. Escobar. *J. Phys. Chem. C*. 2007, **111**, 10799-10805.